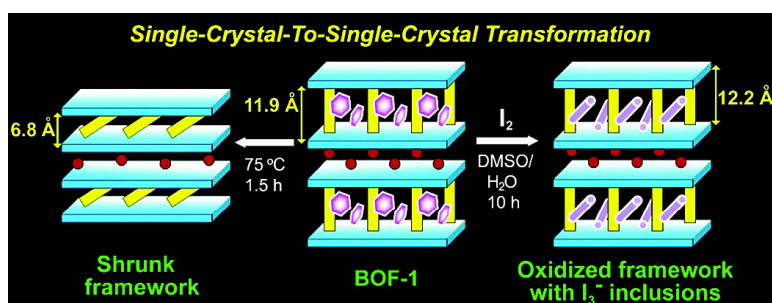# Dynamic and Redox Active Pillared Bilayer Open Framework: Single-Crystal-to-Single-Crystal Transformations upon Guest Removal, Guest Exchange, and Framework Oxidation

Hye Jin Choi, and Myunghyun Paik Suh

More About This Article

Additional resources and features associated with this article are available within the HTML version:

- Supporting Information
- Links to the 14 articles that cite this article, as of the time of this article download
- Access to high resolution figures
- Links to articles and content related to this article
- Copyright permission to reproduce figures and/or text from this article

View the Full Text HTML

Dynamic and Redox Active Pillared Bilayer Open Framework: Single-Crystal-to-Single-Crystal Transformations upon Guest Removal, Guest Exchange, and Framework Oxidation

Hye Jin Choi and Myunghyun Paik Suh*

Contribution from the School of Chemistry, Seoul National University, Seoul 151-747, Republic of Korea

Received June 7, 2004; E-mail: mpsuh@snu.ac.kr

Abstract: A metal-organic pillared bilayer open framework having 3D channels, $[Ni_2(C_{26}H_{52}N_{10})]_3[BTC]_4 \cdot 6C_5H_5N \cdot 36H_2O$ (**BOF-1**, **1**), has been assembled from bismacrocyclic nickel(II) complex $[Ni_2(C_{26}H_{52}N_{10})(Cl)_4] \cdot H_2O$ and sodium 1,3,5-benzenetricarboxylate (Na_3BTC). The channels are occupied by pyridine and water guest molecules. When the single crystal of **1** was dried in air and then heated at 75 °C for 1.5 h, respectively, $[Ni_2(C_{26}H_{52}N_{10})]_3[BTC]_4 \cdot 30H_2O$ (**1′**) and $[Ni_2(C_{26}H_{52}N_{10})]_3[BTC]_4 \cdot 4H_2O$ (**2**) resulted with retention of the single crystallinity. The X-ray structures reveal spongelike dynamic behavior of the bilayer framework that reduces the interlayer distance in response to the amount of guest molecules. Solid **2** differentiates various alcohols. When **1** was immersed in pyridine and benzene, guest molecules were exchanged with retention of the single-crystal nature to give rise to $[Ni_2(C_{26}H_{52}N_{10})]_3[BTC]_4 \cdot 20pyridine \cdot 6H_2O$ (**3**) and $[Ni_2(C_{26}H_{52}N_{10})]_3[BTC]_4 \cdot 14benzene \cdot 19H_2O$ (**4**), respectively. Furthermore, crystal **1** reacted with I_2 via single-crystal-to-single-crystal transformation to produce $[Ni_2(C_{26}H_{52}N_{10})]_3[C_9H_3O_6]_4(I_3)_4 \cdot nI_2 \cdot 17H_2O$ (**5**) that consists of positively charged framework incorporating nickel(III) and nickel(II) ions and the channels including I_3^- and I_2.

Introduction

Metal-organic open frameworks (MOFs) are considered as zeolite analogues, and they have great potential of being applied to adsorption and separation processes,[1−3] ion exchange,[4,5] catalysis,[6,7] and sensor technology.[8,9] MOFs with various structures and topologies have been constructed by using a wide variety of metal ions and organic linkers as building blocks. Modular construction of MOFs by using predesigned molecular building blocks allows control of size, shape, and chemical environment of the voids, which is difficult for zeolites.[10−12]

We have used macrocyclic complexes as metal building blocks because they have fixed vacant coordination sites at the fixed positions, which enables control of the extending direction of networks.[3,13] An exciting yet little explored area is the MOFs that exhibit flexible and dynamic behaviors responding to external stimuli.[2,14] Furthermore, MOFs that are able to alter their framework charge by the redox reaction are extremely rare.[15] If a neutral open framework could be oxidized, it would include free counteranions in the channels or pores, and then it might be applied to anion exchange materials.[4,5] Retaining single crystallinity[16−21] even *after chemical reactions occurred* must be important for the development of certain devices. The phenomenon, however, has never been observed for the redox

(1) (a) Chae, H. K.; Siberio-Perez, D. Y.; Kim, J. H.; Go, Y. B.; Eddaoudi, M.; Matzger, A. J.; O'Keeffe, M.; Yaghi, O. M. *Nature* **2004**, *427*, 523−527. (b) Eddaoudi, M.; Moler, D. B.; Li, H.; Chen, B.; Reineke, T. M.; O'Keeffe, M.; Yaghi, O. M. *Acc. Chem. Res.* **2001**, *34*, 319−330. (c) Eddaoudi, M.; Li, H.; Yaghi, O. M. *J. Am. Chem. Soc.* **2000**, *122*, 1391−1397.
(2) (a) Kitaura, R.; Fujimoto, K.; Noro, S.; Kondo, M.; Kitagawa, S. *Angew. Chem., Int. Ed.* **2002**, *41*, 133−135. (b) Uemura, K.; Kitagawa, S.; Kondo, M.; Fukui, K.; Kitaura, R.; Chang, H.-C.; Mizutani, T. *Chem.—Eur. J.* **2002**, *8*, 3586−3600.
(3) (a) Lee, E. Y.; Suh, M. P. *Angew. Chem.*, *Int. Ed.* **2004**, *43*, 2798−2801. (b) Ko, J. W.; Min, K. S.; Suh, M. P. *Inorg. Chem.* **2002**, *41*, 2151−2157. (c) Min, K. S.; Suh, M. P. *Chem.—Eur. J.* **2001**, *7*, 303−313. (d) Choi, H. J.; Lee, T. S.; Suh, M. P. *J. Inclusion Phenom. Macrocyclic Chem.* **2001**, *41*, 155−162. (e) Choi, H. J.; Lee, T. S.; Suh, M. P. *Angew. Chem.*, *Int. Ed.* **1999**, *38*, 1405−1408.
(4) Min, K. S.; Suh, M. P. *J. Am. Chem. Soc.* **2000**, *122*, 6834−6840.
(5) Yaghi, O. M.; Li, H. *J. Am. Chem. Soc.* **1996**, *118*, 295−296.
(6) Pan, L.; Liu, H.; Lei, X.; Huang, X.; Olson, D. H.; Turro, N. J.; Li, J. *Angew. Chem., Int. Ed.* **2003**, *42*, 542−546.
(7) Sawaki, T.; Aoyama, Y. *J. Am. Chem. Soc.* **1999**, *121*, 4793−4798.
(8) Albrecht, M.; Lutz, M.; Spek, A. L.; van Koten, G. *Nature* **2000**, *406*, 970−974.
(9) Real, J. A.; Andrés, E.; Muñoz, M. C.; Julve, M.; Granier, T.; Bousseksou, A.; Varret, F. *Science* **1995**, *268*, 265−267.
(10) Chui, S. S.-Y.; Lo, S. M.-F.; Charmant, J. P. H.; Orpen, A. G.; Williams, I. D. *Science* **1999**, *283*, 1148−1150.
(11) Eddaoudi, M.; Kim, J.; Rosi, N.; Vodak, D.; Wachter, J.; O'Keeffe, M.; Yaghi, O. M. *Science* **2002**, *295*, 469−472.
(12) Chen, B.; Eddaoudi, M.; Hyde, S. T.; O'Keeffe, M.; Yaghi, O. M. *Science* **2001**, *291*, 1021−1023.
(13) Choi, H. J.; Suh, M. P. *J. Am. Chem. Soc.* **1998**, *120*, 10622−10628.
(14) (a) Fletcher, A. J.; Cussen, E. J.; Prior, T. J.; Rossensky, M. J.; Kepert, C. J.; Thomas, K. M. *J. Am. Chem. Soc.* **2001**, *123*, 10001−10011. (b) Cussen, E. J.; Claridge, J. B.; Rosseinsky, M. J.; Kepert, C. J. *J. Am. Chem. Soc.* **2002**, *124*, 9574−9581.
(15) Oh, M.; Carpenter, G. B.; Sweigart, D. A. *Angew. Chem., Int. Ed.* **2001**, *40*, 3191−3194.
(16) Suh, M. P.; Ko, J. W.; Choi, H. J. *J. Am. Chem. Soc.* **2002**, *124*, 10976−10977.
(17) Atwood, J. L.; Barbour, L. J.; Jerga, A.; Schottel, B. L. *Science* **2002**, *298*, 1000−1002.
(18) (a) Biradha, K.; Fujita, M. *Angew. Chem., Int. Ed.* **2002**, *41*, 3392−3395. (b) Biradha, K.; Hongo, Y.; Fujita, M. *Angew. Chem., Int. Ed.* **2002**, *41*, 3395−3398.
(19) Rather, B.; Zaworotko, M. J. *Chem. Commun.* **2003**, 830−831.
(20) Kepert, C. J.; Rosseinsky, M. J. *Chem. Commun.* **1999**, 375−376.
(21) Maspochi, D.; Ruiz-Molina, D.; Wurst, K.; Domingo, N.; Cavallini, M.; Biscarini, F.; Tejada, J.; Rovira, C.; Veciana, J. *Nat. Mater.* **2003**, *2*, 190−195.

reactions in metal-organic frameworks, although a few inorganic solids showed retention of single crystallinity upon air oxidation.[22]

Previously, we communicated about the synthesis of a bilayer open framework **BOF-1**, which retained its single crystallinity upon removal and exchange of guest molecules.[16] The crystal

$[Ni_2(C_{26}H_{52}N_{10})(Cl)_4]$ + Na₃1,3,5-BTC ⟶ **BOF-1**
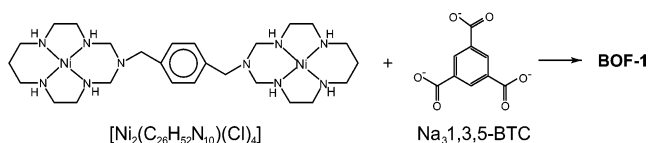
even showed unprecedented spongelike dynamic behavior, reducing the interlayer spacing dramatically in response to the amount of guest molecules. Now, we carried out a redox reaction on the **BOF-1** with I_2 to diversify the function of **BOF-1** from guest recognition to ion exchange. The redox reaction occurred quantitatively on the crystal to give rise to $[Ni_2(C_{26}H_{52}N_{10})]_3$-$[BTC]_4 \cdot nI_2 \cdot 17H_2O$ ($n = 5$ based on elemental analysis and magnetic susceptibility). The compound consists of a positively charged framework containing nickel(II) and nickel(III) macrocyclic complexes with free I_3^- anions and I_2 molecules included in the channels. Even though the redox process involves guest exchange and a ca. 30% increase in the crystal density, it occurs with retention of the single crystallinity. Here, we present properties and X-ray structures of **BOF-1** exhibited by guest removal, guest-exchange, and framework oxidation.

Experimental Section

General Methods. All chemicals and solvents used in the syntheses were of reagent grade and used without further purification. Infrared spectra were recorded with a Perkin-Elmer 2000 FT-IR spectrophotometer. Elemental analyses (EAs) were performed by the analytical laboratory of Seoul National University. NMR spectra were measured on a Bruker AC80 300 MHz FT-NMR spectrometer. UV/vis diffuse reflectance spectra were recorded on a Cary 300 Bio UV/vis spectrophotometer. X-ray powder diffraction (XRPD) data were recorded on a Mac Science M18XHF-22 diffractometer at 50 kV and 100 mA for Cu Kα ($\lambda = 1.540\,50$ Å) with a scan speed of 5°/min and a step size of 0.02°. Thermogravimetric analysis (TGA) and differential scanning calorimetry (DSC) were performed under $N_2(g)$ at a scan rate of 5 °C/min using a Perkin-Elmer TGA7 and DSC7, respectively. EPR spectra were recorded on a Bruker EPR EMX spectrometer. Magnetic susceptibility was measured by a Quantum Design MPMS superconducting quantum interference device (SQUID).

Crystallography. Intensity data for **1**–**5** were collected with an Enraf-Nonius Kappa CCD diffractometer (Mo Kα, $\lambda = 0.710\,73$ Å, graphite monochromator). Preliminary orientation matrices and unit cell parameters were obtained from the peaks of the first 10 frames and were then refined using the whole data set. Frames were integrated and corrected for Lorenz and polarization effects using DENZO.[23] The scaling and the global refinement of crystal parameters were performed by SCALEPACK. No absorption correction was made. The crystal structures were solved by the direct methods[24] and refined by full-matrix least-squares refinement using the SHELXL97 computer program.[25] The positions of all non-hydrogen atoms were refined with

anisotropic displacement factors. The hydrogen atoms were positioned geometrically and refined using a riding model.

Synthesis of $[Ni_2(C_{26}H_{52}N_{10})Cl_4]\cdot H_2O$ (A). To a stirred methanol solution (160 mL) of $NiCl_2 \cdot 6H_2O$ (4.76 g, 20.0 mmol) were slowly added *N,N'*-bis(2-aminoethyl)-1,3-propanediamine (3.30 g, 20.0 mmol), *p*-xylylenediamine (1.38 g, 10.0 mmol), and 37% aqueous formaldehyde (7.17 g, 88.3 mmol). The mixture was heated at reflux for 5 days, during which time the solution gradually became brown. The solution was allowed to stand at room temperature until pink precipitate formed, which was filtered off, washed with methanol, and dried in air. Yield: 25%. The product was recrystallized in H_2O/MeOH to obtain the crystals. Anal. Calcd for $Ni_2C_{26}H_{54}N_{10}Cl_4O$: C, 39.94; H, 6.96; N, 17.91. Found: C, 39.93; H, 6.48; N, 17.79. FT-IR (Nujol mull, cm^{-1}): 3336 (s, br), 3283 (m), 3265 (m), 3212 (s), 1633 (w), 1557 (w).

Preparation and X-ray Diffraction Study of $[Ni_2(C_{26}H_{52}N_{10})]_3$-$[BTC]_4\cdot 6C_5H_5N\cdot 36H_2O$ (BOF-1, 1). To an aqueous solution (7 mL) of **A** (0.600 g, 0.767 mmol) was added dropwise an aqueous solution (3 mL) of Na₃BTC (0.461 g, 1.67 mmol). To the resulting yellow solution was added a mixture of DMSO/pyridine (10 mL, 2:1 v/v) to induce crystallization of the product. The solution was heated and then filtered while hot. The filtrate was allowed to stand at room temperature until pale pink crystals formed, which were filtered off, washed with EtOH, and dried briefly in air. Yield: 78%. Anal. Calcd for $[Ni_2$-$(C_{26}H_{52}N_{10})]_3[BTC]_4\cdot 6C_5H_5N\cdot 36H_2O$ ($Ni_6C_{144}H_{270}N_{36}O_{60}$): C, 45.30; H, 7.13; N, 13.21. Found: C, 45.36; H, 5.50; N, 13.08. FT-IR (Nujol mull, cm^{-1}): 3361 (s), 3156 (s), 1606 (s), 1562 (s), 1365 (s). UV/vis (diffuse reflectance, nm): 510, 645. The X-ray diffraction data of **1** were collected at 100 K for the crystal (0.4 × 0.4 × 0.1 mm³), which was sealed in a glass capillary filled with mother liquor from which **1** was produced (H_2O/DMSO/pyridine: 10:7:3), since the crystal loses guest molecules upon exposure to air.[26]

Preparation and X-ray Diffraction Study of $[Ni_2(C_{26}H_{52}N_{10})]_3$-$[BTC]_4\cdot 30H_2O$ (1′). Single-crystal **1** was allowed to stand in air for 2 h to result in **1′**, and then **1′** was covered with epoxy resin and X-ray diffraction data were collected.

Preparation and X-ray Diffraction Study of $[Ni_2(C_{26}H_{52}N_{10})]_3$-$[BTC]_4\cdot 4H_2O$ (2). The crystal **1** (size 0.2 × 0.2 × 0.1 mm³) was sealed in a glass capillary with mother liquor from which **1** was formed (H_2O/DMSO/pyridine: 10:7:3). After the cell parameters of the crystal were measured to check if they were the same as those of **1**, the crystal was taken out from the capillary, then put on the filter paper, and dried in a programmable oven at 75 °C for 1.5 h. The crystal was picked up, covered immediately with epoxy resin to avoid contact with the moisture from air, and then mounted on the X-ray diffractometer.

Preparation and X-ray Diffraction Study of $[Ni_2(C_{26}H_{52}N_{10})]_3$-$[BTC]_4\cdot 20C_5H_5N\cdot 6H_2O$ (3) and $[Ni_2(C_{26}H_{52}N_{10})]_3[BTC]_4\cdot 14C_6H_6\cdot 19H_2O$ (4). Crystal **1** was sealed in a glass capillary with the mother liquor from which **1** was formed (H_2O/DMSO/pyridine: 10:7:3). After the cell parameters of the crystal were determined, the crystal was taken out from the capillary. Capillaries of 0.5 mm size were filled with pyridine and benzene, respectively. When the capillary was filled with the solvent, an empty space of ca. 1 cm length was made to create two solvent layers. The crystal **1** was dropped into the upper layer of the solvent, and a photograph of the crystal was taken immediately. After the crystal was immersed in the solvent for 24 h, a photograph was taken again to see if the size, morphology, transparency, and position of the crystal were unaltered. Since no change was observed, the possibility of dissolution of **1** in the solvent followed by crystallization or renucleation at the surface and growth of a new phase was excluded. After immersion in the aromatic solvent for 24 h, the crystal was inserted to the empty space created between the two solvent-layers in the capillary by use of a very thin glass fiber, and then the solvent at the upper part of the capillary was taken out. The capillary was cut

(22) (a) Iordanidis, L.; Kanatzidis, M. G. *Angew. Chem., Int. Ed.* **2000**, *39*, 1927–1930. (b) Iordanidis, L.; Kanatzidis, M. G. *J. Am. Chem. Soc.* **2000**, *122*, 8319–8320.

(23) Otwinowsky, Z.; Minor, W. *Processing of X-ray Diffraction Data Collected in Oscillation Mode, Methods in Enzymology*; Carter, C. W., Jr., Sweet, R. M., Eds.; Academic Press: 1996; Vol. 276, pp 307–326.

(24) Sheldrick, G. M. *Acta Crystallogr.* **1990**, *A46*, 467–473.

(25) Sheldrick, G. M. *SHELXL97. Program for the crystal structure refinement*; University of Göettingen: Göettingen, Germany, 1997.

(26) Due to the loss of guest molecules in air, the XRPD pattern of crystal **1** ground in air was almost the same as that of the air-dried sample (**1′**) (see Supporting Information).

into the appropriate size, sealed, and mounted on the X-ray diffractometer. Anal. Calcd for **3** ($Ni_6C_{214}H_{280}N_{50}O_{30}$): C, 58.59; H, 6.45; N, 15.96. Found: C, 56.43; H, 6.33; N, 15.24. Anal. Calcd for **4** ($Ni_6C_{198}H_{290}N_{30}O_{43}$): C, 57.57; H, 7.08; N, 10.17. Found: C, 53.66; H, 7.16; N, 11.77. The microanalysis data for **3** and **4** were unsatisfactory, compared with the calculated values for the formula obtained from the X-ray structures, because pyridine and benzene guest molecules were easily lost from the host framework upon exposure to the atmosphere for the analysis. The found data indicate that six pyridine and five benzene guest molecules were lost per formula unit of **3** and **4**, respectively. Anal. Calcd for $[Ni_2(C_{26}H_{52}N_{10})]_3[BTC]_4 \cdot 14C_5H_5N \cdot 6H_2O$ ($Ni_6C_{184}H_{250}N_{44}O_{30}$): C, 56.51; H, 6.44; N, 15.76. Anal. Calcd for $[Ni_2(C_{26}H_{52}N_{10})]_3[BTC]_4 \cdot 9C_6H_6 \cdot 19H_2O$ ($Ni_6C_{168}H_{260}N_{30}O_{43}$): C, 53.95; H, 7.01; N, 11.23.

Preparation and X-ray Diffraction Study of $[Ni_2(C_{26}H_{52}N_{10})]_3$-$[BTC]_4(I_3)_4 \cdot 5I_2 \cdot 17H_2O$ (5). Single crystals of **1** were immersed in a DMSO/H_2O (1:1 v/v, 2.00 mL) solution of I_2 (0.0136 M) for 10 h. The resulting dark brown crystal was filtered off and washed briefly with water and then ethanol. Anal. Calcd for $Ni_6C_{114}H_{202}N_{30}O_{41}I_{22}$: C, 23.64; H, 3.51; N, 7.25. Found: C, 23.56; H, 2.94; N, 7.41. FT-IR (Nujol mull, cm^{-1}): 3200 (w), 1605 (m), 1553 (m), 1454 (s), 1376 (s), 1170 (w), 1096 (m), 1015 (m), 892 (w), 803 (w), 762 (w), 720 (s). UV/vis (diffuse reflectance, nm): 294, 360 nm. μ_{eff} = 5.26 μ_B (300 K). For X-ray structure determination, crystal **5** (0.3 × 0.3 × 0.1 mm^3) was sealed in a glass capillary together with the mother liquor (I_2 solution in H_2O/DMSO). Intensity data were collected at room temperature.[27] After final refinement, the X-ray data showed high thermal disorder for iodine atoms and large electron residual densities around them. The best refinement was resulted by providing site occupancy factors (sof's) to iodine atoms. All of the sof's for iodine atoms, except two kinds of symmetric triiodide anions, were refined and then fixed as 0.5. For the L-shaped species made of five iodine atoms (I5–I9), the I7···I8 distance was abnormally short for an I_5^- bond, and it was divided into an I_3^- unit (I5–I6–I7) and I_2 unit (I8–I9) by using PART instruction. Some residual electron densities (1.543–1.00 e/$Å^3$) around iodine atoms were not refined for the best refinement results. Even when X-ray data of **5** were collected at 100 K, iodine atoms still exhibited serious thermal disorder. Although one neutral I_2 inclusion was found in the X-ray structure, elemental analysis and magnetic susceptibility data indicated that the compound should have five I_2 molecules per formula unit.

Guest Binding Study for BOF-1 with Various Organic Guests. Pale pink crystals of **1** were dried in a programmable oven at 75 °C for 1.5 h. The solid (11–21 mg) whose weight was exactly measured was immersed in the toluene solutions (5 mL) containing methanol, ethanol, isopropyl alcohol, and benzyl alcohol, respectively, for 2 h at 25 °C. The initial concentrations of methanol, ethanol, iso-propyl alcohol, and benzyl alcohol were varied as 0.0624–1.24 M, 0.0260–0.755 M, 0.0266–0.542 M, and 0.0203–0.359 M, respectively, to keep the saturation (θ) values ranging 20–80%. The concentration changes of the organic guests were measured by GC using dodecane as the internal standard. The GC system was fitted with a 30 m × 0.25 mm × 0.25 μm cross-linked poly(dimethylsiloxane) capillary column and interfaced with a GC ChemStation. The column temperature was programmed from 100 °C (5 min) to 300 °C (2 min) at the rate of 25 °C/min. A flame ionization detector was used. The data were fitted to the equation previously published in our lab to obtain K_f and [BS]o/ω values.[3]

Gas Sorption Measurement. Sorption isotherm study for **BOF-1** was performed using a Quantachrome AUTOSORB-1 sorption instru-

ment. As-synthesized crystals of known weight, which were placed in a cylindrical quartz tube (height, 235.5 mm; diameter, 6 mm), were heated at 130 °C at 10^{-5} Torr for 5.5 h to remove all guest molecules. The N_2 gas (UHP grade) was added incrementally, and the isotherm was recorded at each equilibrium pressure by the static volumetric method. Langmuir surface area and pore volume were estimated using the Langmuir equation and the Dubinin−Radushkevich equation, respectively.

Measurement of Crystal Density. The degree of oxidation of **1**, which depends on the reaction time with I_2 solution, was monitored by the measurement of the crystal density. Typically, the single crystals of **BOF-1** were immersed in 2.00 mL of DMSO/H_2O (v/v 1/1) solution of I_2 (0.0136 M). After a certain reaction time (0.4, 2.5, 2.8, 4.0, 6.8, 9.7 h), a few crystals were picked up and their densities were measured by dropping them in the appropriate solvent whose density was known (0.9−1.7 g/cm^3).

Results and Discussion

Self-Assembly. Our synthetic strategy is to build a bilayer framework generating 3D channels, where 2D coordination polymer layers with cavities are linked together by the flexible pillars. Nickel(II) macrocyclic complexes in square-planar geometry are useful metal building blocks for the design and construction of multidimensional networks, since they have two fixed vacant coordination sites at the trans position,[3,13] which enables control of the extending direction of networks. In addition, they can be oxidized to nickel(III) or reduced to nickel-(I).[28]

To construct a pillared bilayer open framework, we prepared dinickel(II) bismacrocyclic complex $[Ni_2(C_{26}H_{52}N_{10})(Cl)_4] \cdot H_2O$ (**A**) as a metal building block (eq 1), by modifying the one-pot metal-template condensation reactions previously published.[28,29]

$$NiCl_2 \cdot 6H_2O + H_2NCH_2CH_2NH_2 +$$
$$CH_2O + p\text{-}C_6H_4(CH_2NH_2)_2 \rightarrow \mathbf{A} \quad (1)$$
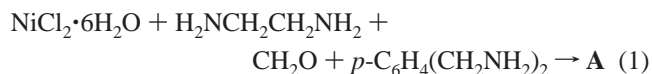
By the self-assembly of **A** and sodium 1,3,5-benzenetricarboxylate (Na$_3$BTC) in water in the presence of DMSO and pyridine, the bilayer open framework $[Ni_2(C_{26}H_{52}N_{10})]_3[BTC]_4 \cdot 6C_5H_5N \cdot 36H_2O$ (**BOF-1**, **1**) was constructed. Although the assembly might yield a 3D network locating **A** alternately in the 2D layers,[30] such architectural isomerism was not observed.

Properties and X-ray Structure of BOF-1 (1). Bilayer framework **1** is insoluble in any organic solvent but slightly soluble in water to decompose into the building blocks. The crystal loses guest water molecules upon exposure to the atmosphere. Thermogravimetric analysis of **1** indicates that all guest molecules can be removed at 135 °C and the solid is stable up to 275 °C.

In the X-ray structure of **1** (Figure 1), each nickel(II) macrocyclic unit of **A** is coordinated with two BTC^{3-} ions at the trans position and each BTC^{3-} ion binds three nickel(II) ions belonging to three different bismacrocyclic units. This results in two 2D layers with the brick-wall motif of size 22.6 × 14.3 $Å^2$. The *p*-xylyl groups of the bismacrocycle act as pillars to link these two layers together. The thickness of bilayer is 11.91(1) Å. The bilayers are closely packed by fitting the grooves together. The framework creates 3D channels, since

(27) Crystal data for **5** ($Ni_6C_{114}H_{202}N_{30}O_{41}I_{14}$): triclinic, space group $P\bar{1}$ with a = 16.434(1) Å, b = 19.914(2) Å, c = 20.338(2) Å, α = 71.255(2)°, β = 70.065(2)°, γ = 74.827(2)°, V = 5837.8(9) $Å^3$, and Z = 1, T = 293 K, d_{calcd} = 1.359 Mg/m^3, $2\theta_{max}$ = 56.72, λ(Mo Kα) = 0.710 73 cm^{-1}, 38 570 reflections measured, 5224 observed ($I > 2\sigma(I)$), 954 parameters, R_1 (unweighted, based on F^2) = 0.1547, R_w = 0.3337. The maximum and minimum peaks on the final difference Fourier map corresponded to 1.543 and −0.902 e/$Å^3$, respectively.

(28) Suh, M. P. *Adv. Inorg. Chem.* **1997**, *44*, 93−146.
(29) Suh, M. P.; Kim, S. K. *Inorg. Chem.* **1993**, *32*, 3562−3564.
(30) Holman, K. T.; Martin, S. M.; Parker, D. P.; Ward, M. D. *J. Am. Chem. Soc.* **2001**, *123*, 4421−4431.
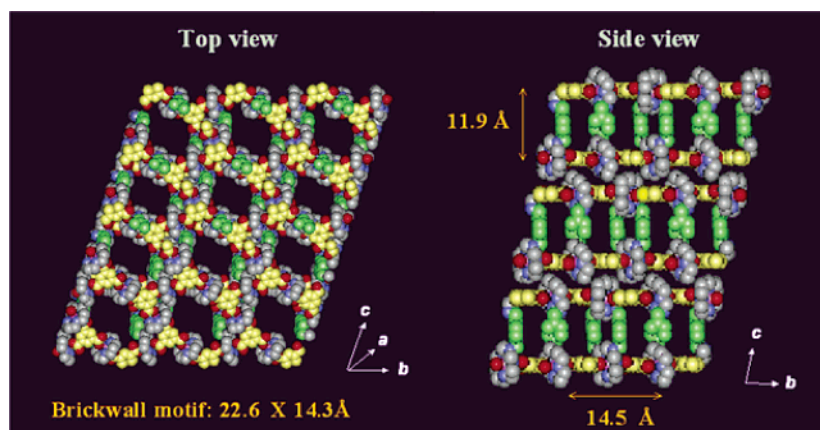
Figure 1. Self-assembly and X-ray structures of **BOF-1** (**1**). (a) Top view showing 2D layers of brick-wall motif. (b) Side view showing pillared bilayer structure [thickness of bilayer, 11.91(1) Å]. Ni, pink; O, red; N, blue; C of macrocycle, gray; C of BTC^{3-}, yellow; C of pillars, green. Guest water and pyridine molecules are omitted for clarity.

the channels are created from top to bottom as well as the side directions. The aromatic rings of *p*-xylyl pillars are positioned regularly almost parallel and perpendicularly to the direction of the side channels with dihedral angles of 1.40°, 87.9°, and 88.4° between them. The channel window size on the side of the bilayer is 14.52(1) Å (the effective channel width corrected for van der Waals surface is 11.12(1) Å). The voids of the channels occupy 61% of the total volume as estimated by PLATON, which are filled with water and pyridine guest molecules.

Spongelike Behavior and Single-Crystal-to-Single-Crystal Transformations of BOF-1 upon Guest Removal. When single-crystal **1** was allowed to stand in air for 2 h, all pyridine and some water guest molecules were removed to yield [Ni$_2$(C$_{26}$H$_{52}$N$_{10}$)]$_3$[BTC]$_4$·30H$_2$O (**1′**). The X-ray structure of **1′** (Figure 2) indicates that there is no change in the 2D layers but the thickness of the bilayer (11.27 Å) is reduced compared with those of **1** (Table 1). When crystal **1** (0.2 × 0.2 × 0.1 mm^3) was dried in a muffle furnace at 75 °C for 1.5 h, transparency of the crystal was slightly lost but the single crystallinity was still maintained to produce [Ni$_2$(C$_{26}$H$_{52}$N$_{10}$)]$_3$[BTC]$_4$·4H$_2$O (**2**). The X-ray data quality of **2** was not as good as that of **1** due to the reduction of transparency. The cell parameters including the cell volume of **2** changed significantly during the transformation from **1** to **2** (Table 1). Although 2D layers in **2** remain intact (cavity size, 22.2 Å × 14.4 Å), the pillars of **2** are greatly tilted and the thickness of the bilayer is dramatically reduced to 6.82(2) Å. The void volume of **2** is 27% of the total volume, as estimated by PLATON (see Figure S3 showing the interior surface of **2** in the Supporting Information). When the single crystal of **2** was exposed to water−pyridine vapor for 12 h or immersed in a water−pyridine mixture for 5 min, it restored structure **1** as evidenced by X-ray powder diffraction patterns (see Supporting Information). However, the crystal was split into too many small pieces to determine the X-ray structure again. When crystal **1** was dried up to 135 °C with a heating rate of 3.8 °C/min, it did not diffract the X-ray beam. However, when the single crystal was dried up to 100 °C with the heating rate of 1.5 °C/m, it showed cell parameters of $a = 11.948(9)$ Å, $b = 16.108(15)$ Å, $c = 19.553(24)$ Å, $\alpha = 74.66(5)°$, $\beta = 88.53(5)°$, $\gamma = 84.46(3)°$, $V = 3612.0(6)$ Å^3, even though the structure refinement was not successful due to the bad quality X-ray data. The completely desolvated framework exhibited the
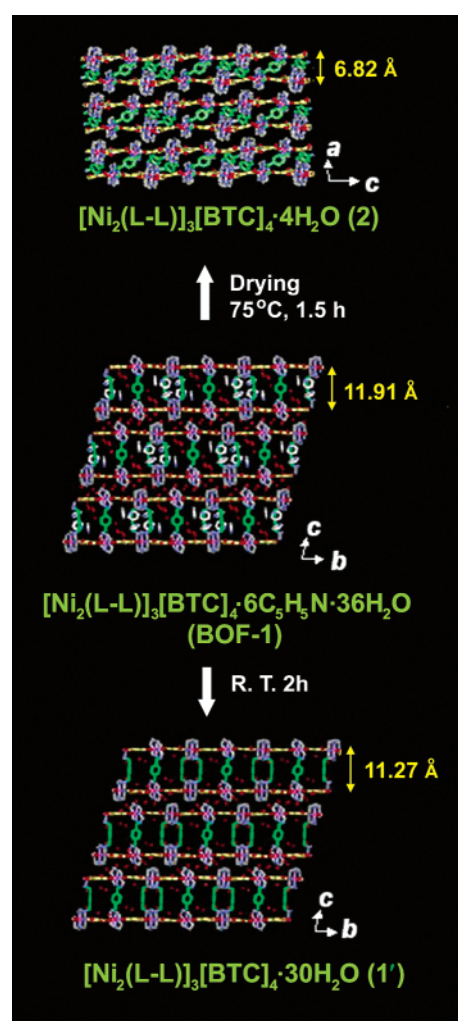

Figure 2. X-ray structures of dried **BOF-1**, exhibiting spongelike behavior.

poor nature of porosity. When **2** was dried further under high vacuum in a gas-sorption apparatus, the N$_2$ gas adsorption isotherm exhibited a Langmuir surface area of 138 m^2/g and pore volume of 0.0876 cm^3/g. In contrast to our intuitive views, **BOF-1** shows a spongelike dynamic behavior responding to the amount of guest molecules, without breaking the single-crystal nature.

Table 1. Crystallographic Parameters for **1**–**5**[a]

compound	1	1′	2	3	4	5
space group	$P\bar{1}$	$P\bar{1}$	$P1$	$P\bar{1}$	$P\bar{1}$	$P\bar{1}$
a, Å	16.505	16.420	12.382	16.467	16.460	16.434
b, Å	19.945	19.817	16.375	20.134	19.849	19.914
c, Å	20.664	20.439	19.952	20.720	20.419	20.338
α, deg	73.00	70.32	74.1	72.53	70.50	71.26
β, deg	68.24	68.55	89.26	67.94	71.08	70.07
γ, deg	76.07	76.19	84.18	75.04	76.30	74.83
V, Å^3	5974.3	5777.9	3877.9	5990.4	5887.0	5837.8
thickness of bilayer, Å	11.91(1)	11.27(2)	6.82(2)	11.71(2)	11.75(2)	12.20(1)

[a] R_1 (unweighted, based on F^2) values are 0.0899 for **1**, 0.1839 for **1′**, 0.1491 for **2**, 0.1279 for **3**, 0.1299 for **4**, and 0.1547 for **5**.
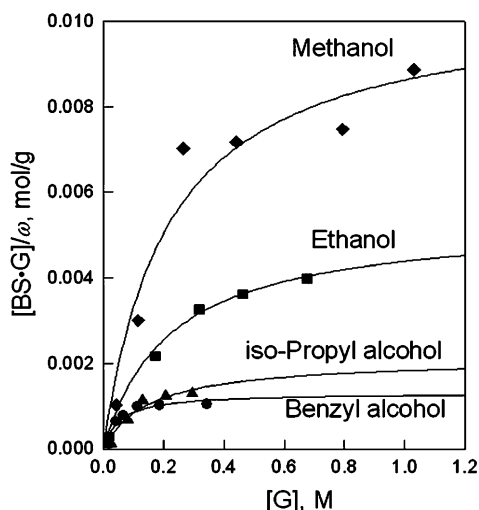

Figure 3. Binding of dried solid **2** (powder form) with guest molecules in toluene.

Table 2. Guest Binding Data for Dried **BOF-1**[a,b]

	K_f, M^{-1}	[BS]$_o/\varpi$, mmol g^{-1}	guest inclusion capacity,[c] mol
MeOH	4.61 ± 1.82	10.5 ± 1.34	29.1
EtOH	4.55 ± 1.31	5.35 ± 0.50	14.8
iso-PrOH	6.49 ± 3.88	2.11 ± 0.58	5.84
BzOH	18.8 ± 8.54	1.31 ± 0.19	3.62

[a] Measurements were performed according to the method in ref 3. [b] K_f and [BS]$_o/\varpi$ indicate the binding constant and the binding capacity of host solid with guest molecules, respectively. [c] Per formula unit of host **2**.

Guest Binding of 2 with Organic Guests. The dried compound **2** that was ground into powder bound methanol, ethanol, iso-propyl alcohol, and benzyl alcohol in toluene, showing Langmuir isotherm curves (Figure 3). The binding constants (K_f) were in the order of benzyl alcohol > isopropyl alcohol > ethanol−methanol, which are summarized in Table 2, together with the maximum number of binding sites for the guest molecules per gram of host solid ([BS]$_o/\varpi$). **BOF-1** binds benzyl alcohol with the greatest K_f value, probably because the phenyl ring of benzyl alcohol involves $\pi-\pi$ interactions with the xylyl pillars of **BOF-1**. As for the amount of guest molecules bound to the host, methanol is the best probably because of its size and hydrogen bond formation with the carbonyl oxygen atoms exposed to the channels of the host.

Single-Crystal-to-Single-Crystal Transformations upon Guest Exchange. BOF-1 is completely insoluble in pyridine and benzene as evidenced by the NMR spectra: after crystals of **1** were immersed for 24 h in d_5-pyridine and d_6-benzene,
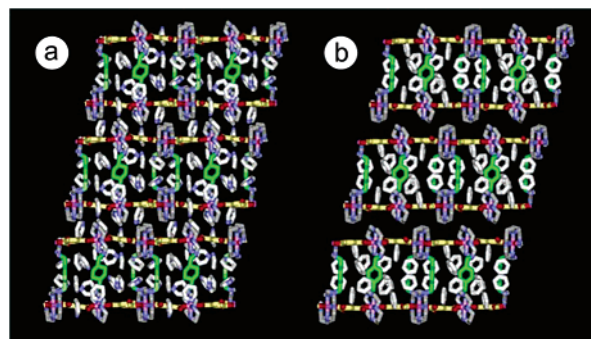
Figure 4. X-ray structures (side views) of **3** (a) and **4** (b). The color codes are the same as those in Figure 1. Organic guest inclusions are indicated as off-white, and water guest molecules are omitted for clarity.
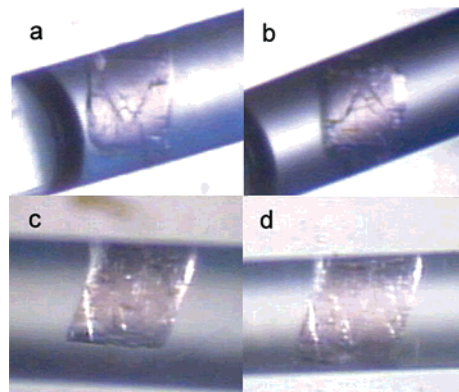
Figure 5. Photographs of **BOF-1** crystal in guest-exchange processes. (a) As soon as **1** was immersed in pyridine within a glass capillary (0.5 mm i.d.). (b) After immersion in pyridine for 24 h. (c) As soon as **1** was immersed in benzene within a glass capillary (0.5 mm i.d.). (d) After immersion in benzene for 24 h.

respectively, the NMR spectra of the d-solvent showed no peak corresponding to the framework of **1**. To determine the X-ray structure of the guest-exchanged crystal, single-crystal **1** was selected and its cell parameters were measured. Then, it was immersed in pyridine or benzene that was filled in a glass capillary (0.5 mm i.d.) for 24 h. The X-ray structures (Figure 4) indicated that some water guest molecules in **1** were exchanged with pyridine and benzene, respectively, to produce $[Ni_2(C_{26}H_{52}N_{10})]_3[BTC]_4 \cdot 20C_5H_5N \cdot 6H_2O$ (**3**) and $[Ni_2(C_{26}H_{52}N_{10})]_3[BTC]_4 \cdot 14C_6H_6 \cdot 19H_2O$ (**4**). During the guest-exchange processes, single-crystal-to-single-crystal transformations took place, retaining the transparency of the crystal. The possibility of dissolution of **1** in the solvent followed by crystallization or renucleation of **3** and **4** at the surface and growth of a new phase is excluded by the photographs taken under the optical microscope during and after immersion of the crystal in the solvent, which showed no change in size, morphology, and transparency (Figure 5). The cell parameters of **3** and **4** are almost the same as those of **1** (Table 1), but R_1 values are extraordinarily high (0.1279 for **3** and 0.1299 for **4**). In **3** and **4**, the size of the brick-wall motif in the 2D layers and the thickness of the bilayer were unaltered, compared to those in **1**. In **3**, pyridine molecules were included in the channels of the framework via face-to-edge $\pi-\pi$ interactions with the phenyl rings of BTC^{3-} of the 2D layers and with the aromatic ring planes of the pillars. They were also intercalated between the bilayer units via hydrogen bonding interactions with the framework. In **4**, benzene molecules were included only in the
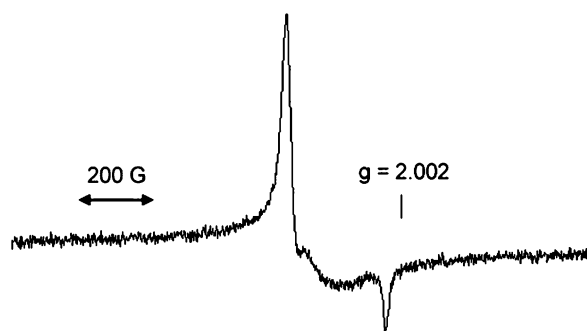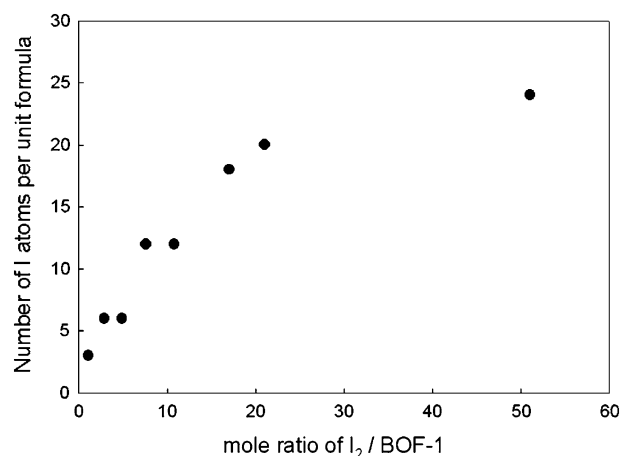
Figure 6. EPR spectrum of **1** (powder sample) measured at room temperature; $g_{\parallel} = 2.024$ and $g_{\perp} = 2.182$.

channels by the $\pi-\pi$ interactions with the host. Benzene inclusion in **BOF-1** was also identified by the NMR spectrum. The crystals of **1** were washed with benzene several times, immersed in benzene (3 mL) for 24 h, then filtered off, and immersed again in DMSO-d_6 (1.5 mL) for 24 h. The NMR spectrum of the DMSO-d_6 showed benzene peaks but no peak corresponding to pyridine molecules that existed in original crystal **1** (see Figure S4 in Supporting Information).

Redox Reaction of BOF-1 with I$_2$ and Properties of 5. Redox reaction was performed on the **BOF-1** with I$_2$ to obtain a positively charged bilayer framework including free counteranions, because the product might be applied to anion exchange.[4,5] When the single crystal ($0.3 \times 0.3 \times 0.1$ mm^3) of **1** was immersed in a DMSO/H$_2$O (1:1 v/v, 2.00 mL) solution of I$_2$ (0.0136 M) for 10 h, the color of the crystal changed from pale pink to dark brown and a redox reaction occurred quantitatively between crystal **1** and I$_2$, which resulted in $[Ni_2(C_{26}H_{52}N_{10})]_3[BTC]_4(I_3)_4 \cdot nI_2 \cdot 17H_2O$ (**5**) ($n = 5$ based on elemental analysis and magnetic susceptibility). By the reaction with I$_2$, two-thirds of the nickel(II) ions contained in the **BOF-1** framework were oxidized to low spin nickel(III) and the I$_2$ molecules were reduced to I$_3^-$ anions, which were included in the channels of the framework. The presence of nickel(III) ions in **5** was characterized by elemental microanalysis, UV/vis diffuse reflectance spectra, and the anisotropic EPR spectrum with the $g_{\perp}$ value being greater than the $g_{\parallel}$ value (Figure 6).[31–33] The variable temperature magnetic susceptibility measurement gave a μ_{eff} value of 5.26 μ_B at 301 K, which corresponded to the estimated 5.29 μ_B for the spin diluted system having four low spin nickel(III) and two nickel(II) ions per formula unit (see Figure S6 in Supporting Information). The unprecedented oxidation of this metal-organic open framework must be attributed to the ability of nickel(II) macrocyclic complex incorporated in the framework to stabilize uncommon nickel(III) oxidation state.[28,31]

The number of free iodine molecules in **1** was determined based on the microanalysis data obtained for the bulk product that was prepared by immersing **BOF-1** crystals in the DMSO–H$_2$O solution of I$_2$ (0.0066 M) for 11 h {Anal. Calcd for Ni$_6$C$_{114}$H$_{202}$N$_{30}$O$_{41}$I$_{22}$: C, 23.64; H, 3.51; N, 7.25. Found: C, 23.80; H, 3.42; N, 7.48. UV/vis (diffuse reflectance): 294, 360 nm}. To obtain **5**, the mole ratio of I$_2$/**BOF-1** should be greater than 20 and the immersion time of **1** in the I$_2$ solution should

(31) Suh, M. P.; Lee, E. Y.; Shim, B. Y. *Inorg. Chim. Acta* **1998**, *269*, 337–341.
(32) Lappin, A. G.; McAuley, A. *Adv. Inorg. Chem.* **1988**, *32*, 241–295.
(33) Marganian, C. A.; Vazir, H.; Baidya, N.; Olmstead, M. M.; Mascharak, P. K. *J. Am. Chem. Soc.* **1995**, *117*, 1584–1594.

Figure 7. Plot of the number of iodine atoms (determined by microanalysis) found in the unit formula of the host [Ni$_2$(C$_{26}$H$_{52}$N$_{10}$)]$_3$[BTC]$_4$ vs mole ratio of I$_2$/**BOF-1** employed in the bulk synthesis. Immersion time of **1** in the I$_2$ solution, 10 h.
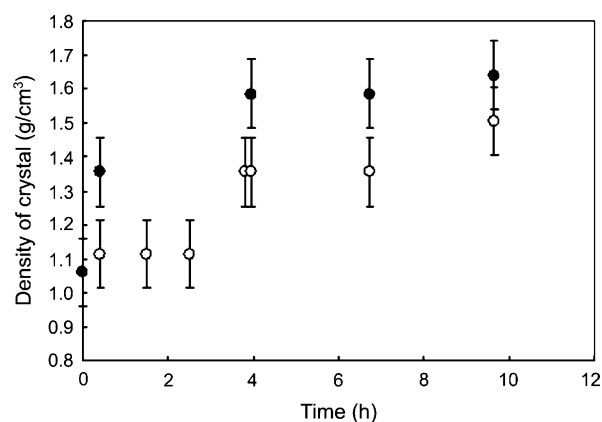
Figure 8. Plot showing the measured density of crystal vs immersion time of the crystal in the DMSO/water (1:1 v/v) (●) and DMSO/CHCl$_3$ (1:1 v/v) solutions of I$_2$ (○). I indicate error range of density.

be longer than 10 h, according to the experimental results shown in Figures 7 and 8. When mole ratio of I$_2$/**BOF-1** was greater than 200, all Ni(II) ions in **BOF-1** were oxidized to the Ni(III) state and [Ni$_2$(C$_{26}$H$_{52}$N$_{10}$)]$_3$[BTC]$_4 \cdot$(I$_3$)$_6 \cdot$(I$_2$)$_2 \cdot$20H$_2$O resulted, which was characterized by the elemental analysis. Its X-ray crystal structure was not determined because of the bad quality X-ray diffraction data.

When single-crystal **BOF-1** was exposed to I$_2$ vapor for 19 h instead of immersion in DMSO–H$_2$O solution or when the dried crystal **2** was exposed to I$_2$ vapor for 55 h, the color of the crystal changed from pale pink to dark brown with retention of the crystal morphology. However, the crystal hardly diffracted the X-ray beam. When a similar reaction was carried out with Br$_2$ in CHCl$_3$ or in EtOH, **BOF-1** was dissolved in the solvent and dissociated into the building blocks, which resulted in a solid of nickel(III) bismacrocyclic complex coordinating Br$^-$ ions at the axial sites {Anal. Calcd for [Ni$_2$(C$_{26}$H$_{52}$N$_{10}$)(Br)$_4$]-[Br]$_2 \cdot$14H$_2$O: C, 23.07; H, 5.95; N, 10.35. Found: C, 23.28; H, 5.70; N, 10.42}.

It should be noted here that **5** could not be directly prepared from the Ni(III) macrocyclic complex and BTC^{3-} in the DMSO/H$_2$O solution because the Ni(III) macrocyclic complex should be isolated only as an octahedral species that has no vacant coordination sites for BTC^{3-}, and moreover the Ni(III) species are easily reduced to Ni(II) in the presence of water.[28]
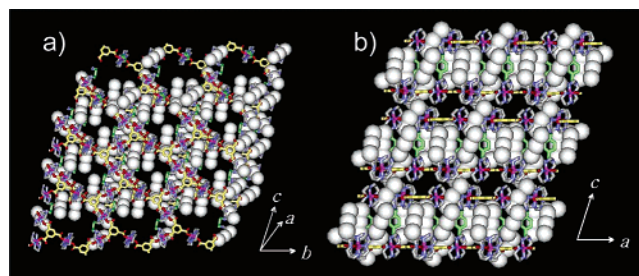
Figure 9. X-ray structure of **5**, showing oxidized framework with I_3^- and I_2 included in the channels. (a) Top view. (b) Side view. Color: Ni, pink; O, red; N, blue; C of macrocycle, gray; C of BTC^{3-}, yellow; C of xyly pillars, green; I, white. Guest water molecules are omitted for clarity.

Figure 10. Photographs showing progress of the redox reaction when a crystal **BOF-1** ($0.5 \times 0.5 \times 0.3$ mm^3) was immersed in the DMSO/H$_2$O (1:1, v/v) solution of I_2 (0.0136 M, 50 μL). The photographs of the crystal showed no further change in color and morphology after 90 min.

Framework **5** is slightly soluble in water. The UV/vis spectrum for the aqueous solution of **5** shows λ_{max} at 283 and 349 nm, which corresponds to the BTC^{3-} and I_3^- species, respectively. This can be compared with the spectrum of the aqueous solution of CsI$_3$ that shows λ_{max} = 287 nm (ϵ = 3100 cm^{-1} M^{-1}) and 345 nm (ϵ = 1910 cm^{-1} M^{-1}) as well as the spectrum of Na$_3$BTC showing λ_{max} at 283 nm (ϵ = 304 cm^{-1} M^{-1}). The solubility of **5** in water is ca. 7%, as estimated by the absorption intensity of I_3^- at 349 nm. When the solid **5** was immersed in MeOH, EtOH, DMF, or acetone, where the solid was completely insoluble, the solvent became yellow (λ_{max} = 290 and 358 nm). In addition, when it was immersed in CHCl$_3$, the solvent became purple (λ_{max} = 510.2 nm). These indicate that I_2 guest molecules are dissociated from the solid upon immersion in the organic solvents. TGA/DSC data indicate that all water molecules and an iodine guest are removed at 250 °C, and then the framework starts to decompose.

X-ray Structure of [Ni$_2$(C$_{26}$H$_{52}$N$_{10}$)]$_3$[BTC]$_4$(I$_3$)$_4$·nI$_2$·17H$_2$O (5): Single-Crystal-to-Single-Crystal Transformation upon Redox Reaction. During the redox process of **BOF-1** with I_2, single-crystal-to-single-crystal transformation occurred, and the X-ray structure of **5** was able to be determined. The X-ray structure of **5** is shown in Figure 9. The X-ray structure of **5** indicates a positively charged framework and I_3^- counteranions included in the channels. In **5**, two-thirds of nickel atoms are nickel(III). The crystallographic inversion center is located at the center of the bridging xylyl group of the bismacrocycle, and thus two nickel ions belonging to the same bismacrocyclic complex have the same oxidation state. The Ni–N and Ni–O bond distances involving nickel(III) are shorter than those involving nickel(II) ions: av Ni(III)–N and Ni(III)–O bond distances, 1.966(6) Å and 2.103(6) Å; av Ni(II)–N and Ni(II)–O bond distances, 2.000(8) Å and 2.130(8) Å, respectively. The bond distances are compared with those of **BOF-1** (av Ni(II)–N and Ni(II)–O bond distances, 2.054(1) Å and 2.196(3) Å, respectively). As for the included counteranions, the crystallographic asymmetric unit of **5** contains four independent half units of I_3^- and one-half unit of I_2. The I–I distances for two kinds of symmetric I_3^- are 2.923(2) Å (I1–I3) and 2.912(2) Å (I2–I4) with I–I–I angles of 180.00°. Another two half units of I_3^- have asymmetric I–I distances of 2.876(13) Å (I5–I6) and 2.850(10) Å (I6–I7) with an angle of 174.6(4)° (I5–I6–I7) and 2.653(17) Å (I10–I11) and 3.245-(0.023) Å (I11–I12) with an angle of 164.3(1.4)° (I10–I11–I12).[34] A half unit of I_2 has an I–I distance of 2.70(2) Å. Intermolecular distances between iodide species are 4.642 Å for I3···I7 ($x + 1$, $y - 1$, z), 4.754 Å for I4···I9 ($-x$, $-y + 1$,
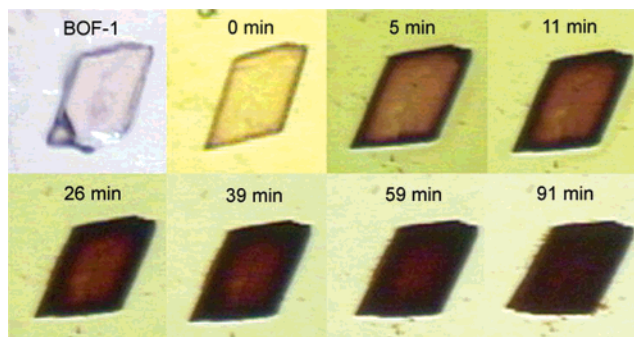
$-z$), and 4.012 Å for I6···I8. Recently, a Cu(II) coordination polymer that includes L-shaped I_5^- anions has been reported.[35] In this case, the I_5^- ion was formed by the I^- ion linked with two I_2 molecules. Even though many I_3^- ions were introduced into the channels of **5**, the thickness of bilayer (12.20(1) Å) was very little changed compared with that of **BOF-1** (11.91(1) Å). The cell parameters were not significantly altered either, compared with those of **BOF-1** (Table 1), although the density of the redox product **5** (1.359 g/cm^3) increased remarkably (ca. 28%) relative to that (1.061 g/cm^3) of **BOF-1**.

Photographs were taken of the crystal of **BOF-1** ($0.5 \times 0.5 \times 0.3$ mm^3) during the reaction with the I_2 solution (Figure 10) to prove the single-crystal-to-single-crystal transformation and exclude the possibility of dissolution and recrystallization. According to the photographs, I_2 inclusion starts at the crystal surface and diffuses into the center of the crystal. Because of the existence of 3D channels in the framework, water inclusions could come out of the channels without interrupting the incoming I_2 molecules. Therefore, the crystal experiences little physical stress during the exchange of water guests with I_2 molecules, which must be followed by the redox reaction between the host and I_2 guests. This enables the crystal to retain the single-crystal nature. Recently, it has been reported that diffusion of I_2 vapor into the crystal of tris(*o*-phenylenedioxy)-cyclotriphosphazene constructs a wirelike confinement of I_2 in the 1D channels of the host.[36] This is different from the present result that redox reaction occurs between the host and I_2 guest.

The diffusion coefficient (*D*) of I_2 in the present **BOF-1** crystal was estimated to be 9×10^{-9} cm^2/s based on the results that $0.3 \times 0.3 \times 0.1$ mm^3 size of the crystal was completely oxidized by I_2 within 10 h. This is significantly greater than the value ($D = 10^{-11}-10^{-10}$ cm^2/s) generally accepted for the metal-organic open frameworks.[14] For zeolites, *D* ranges from 10^{-14} to 10^{-5} cm^2/s, depending on the geometry and dimension of the channels as well as size and shape of the guest molecule, etc..[37] The fast diffusion in the present compound must be attributed to the 3D channels created in the **BOF-1** framework. The material may be a good ion-conductor and/or a good ion-exchange material. However, **5** cannot be applied to an anion-

(34) CSD database released on April, 2002. Allen, F. H.; Kennard, O. *Chemical Design Automation News* **1993**, *8* (1), 1 and 31–37.
(35) Lu, J. Y.; Schauss, V. *Eur. J. Inorg. Chem.* **2002**, 1945–1947.
(36) Hertzsch, T.; Budde, F.; Weber, E.; Hulliger, J. *Angew. Chem., Int. Ed.* **2002**, *41*, 2281–2284.
(37) Bhatia, S. *Zeolite Catalysis: Principles and Applications*; CRC press Inc.: Florida, 1990; Chapter 4, pp 49–74.

exchange material in the present state because it is slightly soluble in H_2O. The modification of the solubility is currently under way.

In conclusion, **BOF-1**, a pillared bilayer framework with 3D channels, serves as molecule recognition material. It shows spongelike dynamic behavior in response to the amount of guest. It exhibits single-crystal-to-single-crystal transformations upon the guest removal and the exchange processes. **BOF-1** reacts with I_2 solution to give rise to a charged framework incorporating Ni(II) and Ni(III) ions with free I_3^- and I_2 inclusions. During the harsh redox reaction that accompanies guest-exchange and ca. 30% increase in the crystal density, the framework still maintains a single-crystal nature. The design may be applied to prepare a new class of versatile multifunctional crystalline materials, including host lattices for optoelectronic materials, molecular separation, and chemical reactions in nanoscale voids.

Supporting Information Available: TGA/DSC data of **1**, XRPD patterns of **1** and **2**, and ORTEP drawing, tables of X-ray data, and X-ray crystallographic files in CIF format for **5**. This material is available free of charge via the Internet at http://pubs.acs.org.

JA0466715